Equilibrium and Kinetic Analysis of Folding of Ketosteroid Isomerase from *Comamonas testosteroni*†

Do-Hyung Kim,[‡,§] Do Soo Jang,[‡] Gyu Hyun Nam,[‡] Sunggoo Yun,[§,||] Jae Hyun Cho,[‡] Gildon Choi,[‡] Hee Cheon Lee,[§,||] and Kwan Yong Choi*[,‡,§]

Division of Molecular and Life Sciences, Center for Biofunctional Molecules, and Department of Chemistry, Pohang University of Science and Technology, Pohang, 790-784, Republic of Korea

Received April 17, 2000; Revised Manuscript Received August 8, 2000

ABSTRACT: Equilibrium and kinetic analyses have been carried out to elucidate the folding mechanism of homodimeric ketosteroid isomerase (KSI) from *Comamonas testosteroni*. The folding of KSI was reversible since the activity as well as the fluorescence and CD spectra was almost completely recovered after refolding. The equilibrium unfolding transitions monitored by fluorescence and CD measurements were almost coincident with each other, and the transition midpoint increased with increasing protein concentration. This suggests that the KSI folding follows a simple two-state mechanism consisting of native dimer and unfolded monomer without any thermodynamically stable intermediates. Sedimentation equilibrium analysis and size-exclusion chromatography of KSI at different urea concentrations supported the two-state model without any evidence of folded monomeric intermediates. Consistent with the two-state model, ^{1}H-^{15}N HSQC spectra obtained for KSI in the unfolding transition region could be reproduced by a simple addition of the spectra of the native and the unfolded KSI. The KSI refolding kinetics as monitored by fluorescence intensity could be described as a fast first-order process followed by a second-order and a subsequent slow first-order processes with rate constants of 60 s^{-1}, 5.4 × 10^{4} M^{-1}·s^{-1}, and 0.017 s^{-1}, respectively, at 0.62 M urea, suggesting that there may be a monomeric folding intermediate. After a burst phase that accounts for >83% of the total amplitude, the negative molar ellipticity at 225 nm increased slowly in a single phase at a rate comparable to that of the bimolecular intermediate step. The kinetics of activity recovery from the denatured state were markedly dependent upon the protein concentration, implying that the monomers are not fully active. Taken together, our results demonstrate that the dimerization induces KSI to fold into the complete structure and is crucial for maintaining the tertiary structure to perform efficient catalysis.

Δ^{5}-3-Ketosteroid isomerase (KSI)[1] from *Comamonas testoseroni* is an enzyme catalyzing the allylic rearrangement of a variety of Δ^{5}-3-ketosteroids to Δ^{4}-3-ketosteroids, shifting a double bond from the 5(6)-position to the 4(5)-position (Scheme 1) (*1*). KSI is one of the most proficient enzymes, enhancing the catalytic rate by a factor of 11 orders of magnitude compared with the corresponding nonenzymatic reaction (*2*). The enzyme has been studied extensively as a prototype to understand the enzyme mechanism of the allylic rearrangement (*3*−*7*).

Recent determinations of the X-ray crystal structures as well as the NMR solution structures have contributed significantly to the understanding of the active site geometry for efficient catalysis (*8*−*11*). One of the most interesting

Scheme 1

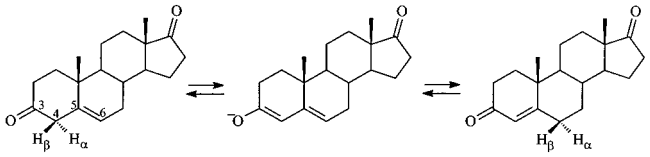

structural features of KSI is that it is a homodimeric enzyme. KSI is folded into a six-stranded β-sheet and three α-helices in each monomer (*10*) (Figure 1). The homologous isozyme from *Pseudomonas putida* biotype B with 34% amino acid identity also exhibited the same tertiary fold as *C. testosteroni* KSI (*8*). Each monomer forms one complete active site consisting of the residues from the same monomer, not from the partner monomer. The KSI monomers interact with each other over a narrow and long patch of β-sheet of each monomer (*10*, *11*). The interface between the subunits is well-defined and is formed between the convex surfaces of the β-sheets. Each subunit buries approximately 1300 Å^{2} on formation of the dimer, indicating that the dimeric interaction is extensive to provide many favorable interactions. These extensive dimeric interactions of KSI point to potential contributions of dimerization to the function and stability of this enzyme.

† This work was supported by a grant from the Korea Science and Engineering Foundation and in part by the Brain Korea 21 Project.

* To whom correspondence should be addressed. Tel: 82-54-279-2295. Fax: 82-54-279-2199. E-mail: kchoi@postech.ac.kr.

‡ Division of Molecular and Life Sciences.

§ Center for Biofunctional Molecules.

|| Department of Chemistry.

[1] Abbreviations: KSI, ketosteroid isomerase; pSK(−), pBluescript SK(−); EDTA, ethylenediaminetetraacetic acid; CD, circular dichroism; NMR, nuclear magnetic resonance; HSQC, heteronuclear single quantum correlation; $\Delta G_{U}^{H_2O}$, Gibbs free energy change for unfolding in the absence of urea and at 25 °C; 5-AND, 5-androstene-3,17-dione.

10.1021/bi000872d CCC: $19.00
Published on Web 09/26/2000

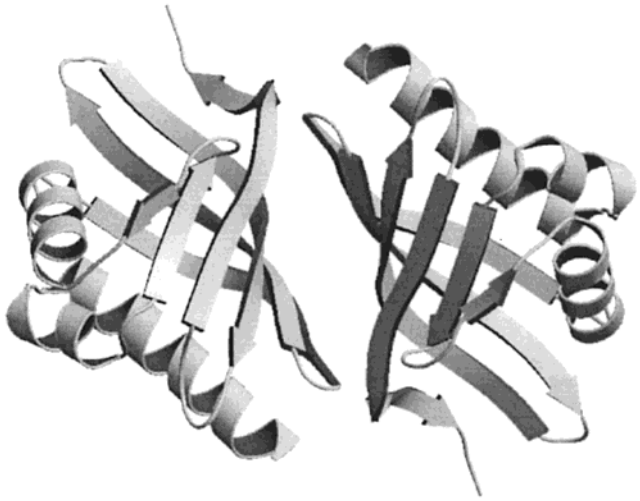

FIGURE 1: Ribbon diagram of the three-dimensional structure of *C. testosteroni* KSI dimer (*10*). Each monomer consists of three α-helices and six β-strands. The program Molscript (*12*) was used for drawing the figure.

Dimerization is commonly found in many enzymes, even in the case where each subunit contains all the functional groups necessary for catalysis. In the case of triosephosphate isomerase, the monomer was not fully active and less stable, emphasizing the importance of dimerization in function and stability (*13*, *14*). The disruption of the quaternary structure of superoxide dismutase was created by mutation of some residues in the interface region, but this monomeric form had a much lower activity than the native dimeric species (*15*). Dimerization also plays an important role in folding of dimeric proteins (*16*−*18*). Studies on the folding mechanism of such dimeric proteins as *E. coli* Trp repressor (*19*), P22 Arc repressor (*20*), and p53tet repressor (*21*) have contributed to better understanding of the role of long-range interactions in protein folding. In the case of KSI, the KSI dimer was unusually stable to dissociation upon dilution even at concentrations near nanograms per milliliter (*22*−*24*). Even though this observation suggests that the dimerization is important for the structural stability of KSI, it is not clear whether a monomeric form is able to exist or how much the dimeric interaction contributes to the active-site geometry for efficient catalysis. Furthermore, the extensive hydrophobic interactions at the dimeric interface imply a potential role of the dimeric interaction in the folding of the monomeric structure.

In this study, we report the results of both equilibrium and kinetic studies on the folding of *C. testosteroni* KSI. The equilibrium unfolding transition was monitored by CD and fluorescence intensities of KSI at different urea concentrations. Our results showed that the equilibrium unfolding follows a simple two-state mechanism involving only the native dimer and the unfolded monomer. The two-state mechanism was supported in different ways by utilizing ^{1}H-^{15}N HSQC spectroscopy, sedimentation equilibrium ultracentrifugation, and size-exclusion chromatography. The kinetic analysis of refolding exhibited a fast first-order process followed by a second-order process and a slow first-order process, suggesting that a monomeric folding intermediate might occur prior to the dimerization. Monitoring the ellipticity change at 225 nm during refolding revealed that the secondary structure might form at a very early stage. The protein concentration dependence of the full activity recovery was analyzed to estimate the activities of the monomers. Our studies provided a valuable insight into the roles of dimerization in stability, folding, and catalysis of KSI.

EXPERIMENTAL PROCEDURES

Reagents and Experimental Conditions. Chemicals for buffer solutions, deoxycholate, and ultrapure urea were purchased from Sigma. 5-Androstene-3,17-dione (5-AND) was purchased from Steraloids. The Superose 12 gel filtration column was obtained from Amersham Pharmacia Biotech. The temperature was maintained at 25 °C for all experiments. The protein concentration was determined based on the difference spectrum change at 295 nm as described previously (*25*).

Protein Source and Purification. The wild-type KSI of *C. testoseroni* was overexpressed in *Escherichia coli* BL21-(DE3) containing pKSI-TI (*10*), an expression vector carrying the wild-type gene of *C. testosteroni* KSI, and purified to homogeneity by deoxycholate affinity chromatography and Superose 12 gel filtration chromatography according to the methods described previously (*26*). The homogeneity of the protein was confirmed by the presence of a single band on SDS−polyacrylamide gels stained with Coomassie blue.

Fluorescence and CD Spectra. The fluorescence spectra of the native, denatured, and refolded enzymes were obtained by use of a fluorescence spectrophotometer (Photon Technology International) equipped with a photomultiplier detector system. With the excitation wavelength at 275 nm, the emission spectrum was monitored in the range from 279 to 450 nm. The bandwidths for the excitation and emission wavelengthes were 2 nm. The step resolution and the integration time were 1 nm and 1 s, respectively. The denatured enzyme was obtained by incubating the enzyme in a buffer solution containing 20 mM potassium phosphate, pH 7.0, and 7 M urea. The refolded enzyme was prepared by diluting the denatured enzyme into the urea concentration of 0.27 M. The final enzyme concentrations were 15 μM. Three independent measurements were averaged for analysis.

The CD spectra of the native, denatured, and refolded enzymes were also obtained by use of a spectropolarimeter (Jasco 715). A cuvette with 0.2 cm path length was used for all spectral measurements. The CD spectra were obtained with a scan speed of 20 nm/min and a bandwidth of 2 nm. Scans were collected at 0.2 nm intervals with a response time of 0.25 s and accumulated 3 times. All the CD spectra were corrected by subtracting the spectrum of the buffer solution. The secondary structural contents were estimated from the spectra of the native and refolded proteins utilizing the ContinLL (*27*) and CDsstr programs (*28*). The reference sets containing 29 or 48 proteins were used for the estimation.

Equilibrium Unfolding. KSI (15 μM) was preincubated in a buffer containing 25 mM phosphate, pH 7.0, 0.5 mM EDTA, and 0−8 M urea longer than 48 h. The fluorescence intensity of KSI was measured by use of a fluorescence spectrophotometer (Shimadzu model RF-5000) equipped with a thermostatically controlled cell holder. With the excitation wavelength at 275 nm, the emission fluorescence intensity at 304 nm was monitored for the proteins incubated at different urea concentrations. The ellipticity at 222 nm

was also monitored by use of a spectropolarimeter (Jasco 715).

The changes in the optical properties of the protein were compared by normalizing each transition curve to the apparent fraction of the unfolded form, F_U:

$$F_U = (Y_N - Y)/(Y_N - Y_U) \quad (1)$$

where Y is the observed fluorescence intensity or molar ellipticity at a given urea concentration and Y_N and Y_U are the observed values for the native and unfolded forms, respectively, at the same denaturant concentration. A linear dependence of Y on denaturant concentration was observed in the baseline regions of the native and unfolded states for both fluorescence and CD spectroscopic methods. Linear extrapolations from these baselines were made to obtain estimates of Y_N and Y_U in the transition region.

The equilibrium constant (K_U) and free-energy change (ΔG_U) for the denaturation were determined according to a two-state model of denaturation by utilizing the following equations (*29*):

$$K_U = 2P_T[F_U{}^2/(1 - F_U)] \quad (2)$$

$$\Delta G_U = -RT \ln(K_U) = \Delta G_U{}^{H_2O} - m[\text{urea}] \quad (3)$$

where P_T is the total protein concentration, $\Delta G_U{}^{H_2O}$ is the free-energy change in the absence of urea, and m represents a measure of the ΔG_U dependence on urea concentration. The data of a urea denaturation curve were fitted to eq 4 (*29*) by a nonlinear least-squares analysis using a nonlinear least-squares program, Kaleidagraph version 2.6 (Abelbeck Software).

$$F_U = \exp[(m[\text{urea}] - \Delta G_U{}^{H_2O})/RT]\{\{1 + 8P_T/\exp[(m[\text{urea}] - \Delta G_U{}^{H_2O})/RT]\}^{1/2} - 1\}/4P_T \quad (4)$$

Sedimentation Equilibrium Experiments. The oligomeric state of KSI at different urea concentrations was determined by sedimentation equilibrium analysis with an ultracentrifuge (Beckman XL-A) at 25 °C. The protein concentration was 15 μM. The protein was incubated for longer times than 48 h in a buffer containing 20 mM potassium phosphate, pH 7.0, and urea at various concentrations. Spectroscopic absorbances were then obtained at two wavelengths, 230 and 280 nm, with a rotor speed of 27 000 rpm. The absorbances were plotted in logarithmic scale against the radius squared to compare the relative slopes of the plots at different urea concentrations. The partial molar volume of KSI and solvent densities at different urea concentrations were calculated as described previously (*30*).

Gel-Filtration Chromatography of KSI in Urea. KSI (50 μM) was incubated at room temperature longer than 48 h in various concentrations of urea at 0, 4, and 6 M, respectively. The incubated samples were then loaded onto a Superose 12 gel filtration column equilibrated previously with a buffer containing 40 mM potassium phosphate, pH 7.0, 1 mM EDTA, 20 mM β-mercaptoethanol, and urea at the respective concentration of 0, 4, or 6 M. The column was eluted with the buffer at a flow rate of 0.4 mL/min. The absorption peak was monitored at 280 nm with a UV-absorbance detector (Amersham Pharmacia Biotech, Uvicord II). The elution time was compared with those of blue-dextran (2000 kDa), ovalbumin (45 kDa), and RNase A (14 kDa).

Expression and Purification of Labeled KSI. A single colony of *E. coli* BL21(DE3)(pLysS) (Novagen, Madison, WI) containing pKSI-TI (*10*) was inoculated in 5 mL of M9 minimal medium, and grown at 37 °C for 15−20 h. A 1.5 mL sample of the culture was transferred to 50 mL of the minimal medium and then incubated at 37 °C for 10 h. The cultures were diluted 50-fold into M9 medium supplemented with 0.1% (w/v) ^{15}N-labeled NH_4Cl (Cambridge Isotope Laboratories, Inc., 99% ^{15}N) and 2×10^{-4}% (w/v) thiamin and biotin, and then grown at 37 °C until the absorbance at 600 nm reached 0.7. After addition of isopropyl α-thiogalactopyranoside to a final concentration of 0.6 mM, the cells were further incubated for 5 h. The labeled protein was collected by centrifugation and purified according to the procedure described above.

HSQC Spectra. The NMR sample was prepared to contain 1 mM KSI in 90% H_2O and 10% ^2H_2O (v/v) at pH 7.0 after adjusting the urea concentration. NMR spectra were collected on an NMR spectrometer (Bruker DRX500) equipped with a triple resonance, pulse field gradient probe with actively shielded z-axis gradients. Larmor frequencies were 500.13 and 50.68 MHz for ^{1}H and ^{15}N, respectively. The ^{1}H chemical shifts were determined relative to that of sodium 2,2-dimethyl-2-silapentane-5-sulfonate (DSS) since it was reported to be insensitive to temperature change. Indirect referencing was adopted for determining ^{15}N chemical shifts by use of the frequency ratio of DSS in water (ω_N/ω_H), 0.101329118 (*31*). Two-dimensional ^{1}H-^{15}N heteronuclear single quantum correlation (HSQC) spectra were obtained using sensitivity-enhanced pulse sequences (*32*) that include the pulse field gradient to select the coherence transfer pathway and to suppress solvent signal. All spectra were recorded with spectral widths of 2500 Hz over 2048 complex points in the t_2 dimension and 2280 Hz over 128 complex points in the t_1 dimension. The relaxation delay of 2.7 s was employed, and 24 transients were accumulated per t_1 increment. The carrier frequency of ^{1}H was placed on the center position of amide peaks (8.2 ppm), and ^{15}N was set to 120 ppm in order to exclude the urea and water signal in the detection region. ^{15}N decoupling during the detection period was employed with the use of a WALTZ decoupling sequence using a 2 kHz radio frequency field (*33*). Quadrature detection in the ω_1 dimension was obtained by use of the States method (*34*). The data were processed on a workstation (Silicon Graphics IndyPC) using the program XWIN NMR (Bruker Co.). To increase the signal-to-noise ratio, all spectra were processed using exponential multiplication (line broadening = 5 Hz) in the t_2 dimension. In the t_1 dimension, zero-filling was used to obtain 256 data points, and a 90° phase-shifted sine bell window function was applied prior to Fourier transformation and baseline correction.

Stopped-Flow Experiments for Refolding Kinetics. Refolding kinetic experiments were performed on a stopped-flow instrument (Bio-Logic SFM-4/QS). Fifty microliters of the protein solution in 8 M urea at pH 7.0 was mixed with 600 μL of the buffer containing 20 mM potassium phosphate at pH 7.0 by use of a built-in mixing apparatus. The final urea concentration was 0.62 M in the refolding condition. To enhance the mixing efficiency with urea, a mixer (Bio-Logic

HDS) was mounted in front of the sample cuvette (Bio-Logic FC-20). During the refolding process, the fluorescence intensity passing through the 295 nm cutoff filter (Oriel) was measured after excitation at 275 nm. The light source was a Xe/Hg lamp, and a monochromator was adjusted to set the wavelength at 275 nm. The emission fluorescence was amplified by use of a photomultiplier supplied with a high voltage at 800 V. The dead time of the instrument was 8 ms. The fluorescence change was recorded with a sampling time of 1 ms. Four different protein concentrations, 0.8, 1, 2, and 4 μM, were tried to analyze the dimerization step in the folding process. The ellipticity change at 225 nm was also monitored during refolding by use of the Bio-Logic stopped-flow instrument equipped with a photoelastic modulator (PEM-90, HINDS Instruments, Inc.). The refolding condition was identical to that for the fluorescence measurement. The light source was a Xe/Hg lamp, and the signal was amplified by a photomultiplier supplied with a high voltage at 260 V. The dead time of the instrument for the ellipticity measurement was 8 ms. The ellipticity change was recorded with a sampling time of 20 ms.

The rate constants were obtained by fitting the data to the following equation:

$$F_t = F_\infty + \sum F_i[1 - \exp(-k_i t)] \qquad (5)$$

where F_t is the signal at time t, F_∞ is the signal of the final state, F_i is the amplitude of the kinetic phase, and k_i is the rate constant for refolding. Data fitting was carried out using the Kaleidagraph program.

Measurement of Half-Time for Recovery of Activity from the Denatured State. The enzyme activity was determined for the protein refolded from the denatured state. The unfolded protein in 7 M urea solution was diluted into 3 mL of the assay buffer containing 34 mM potassium phosphate, 2.5 mM EDTA, pH 7.0, and 116 μM 5-AND. The final urea concentration was 0.0233 M. The absorbance was monitored at 248 nm during the refolding process by use of a spectrophotometer (Cary 3E). The half-time was taken as the time at which the slope of the absorbance change reached the half of the final slope. The half-time was determined at enzyme concentrations in the 10−40 nM range.

RESULTS

Reversibility of Folding. The reversibility of folding was tested by comparing the fluorescence spectrum of the refolded protein with that of the native protein. The spectrum of the native protein exhibited maximum fluorescence intensity at 302 nm when the protein was excited at 275 nm (Figure 2). This spectral pattern is an expected one since KSI contains three tyrosine residues and no tryptophan residue. When the protein was unfolded in the 7 M urea solution, the fluorescence spectrum of the denatured protein exhibited a maximum emission band at 303 nm matching that of a free tyrosine. The fluorescence intensity of the denatured protein was about 2 times lower than that of the native protein near the maximum wavelength. Refolding of KSI was induced by diluting the denatured protein to decrease the urea concentration down to 0.27 M. The refolding was not instantaneous but required about 20 min to reach equilibrium. The fluorescence spectrum of the refolded protein was almost similar to that of the native protein with the recovery of the fluorescence intensity to the level of the native protein. This observation suggests that the refolded protein contains almost the same tertiary structure as the native protein.

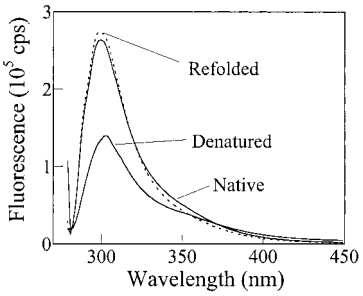

FIGURE 2: Comparison of the fluorescence spectra of native, denatured, and refolded KSI. The spectra were obtained after excitation at 275 nm. The concentration of KSI was 15 μM for all the samples. The protein was dissolved in buffer containing 20 mM potassium phosphate, pH 7.0, with or without 7 M urea for the native or denatured protein, respectively. To prepare the refolded protein, the denatured protein was diluted into phosphate buffer to have a final urea concentration of 0.27 M and incubated longer than 48 h for equilibration.

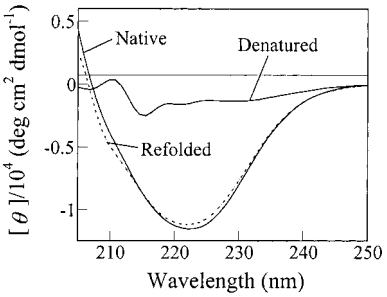

FIGURE 3: Comparison of the circular dichroism spectra of the native, denatured, and refolded KSI. The protein samples were prepared as described in the legend of Figure 2. The CD spectra were obtained with a scan speed of 20 nm/min and a bandwidth of 2 nm. Scans were collected at a step resolution of 0.2 nm with a response time of 0.25 s and accumulated 3 times. All the CD spectra were displayed relative to those of the used buffers. The *y*-axis represents the mean residue molar ellipticity obtained using the protein concentration, the path length, and the residue number of the protein. The spectra were smoothed by a program supplied by the manufacturer of the spectrometer (JASCO).

The CD spectrum of the native protein exhibited a typical pattern of α/β proteins with α-helix and β-strand contents of 29.6% and 25.6%, respectively, on average, when the spectrum was analyzed by the ContinLL and CDsstr programs (*27*, *28*) (Figure 3). The α-helical content agreed well with the X-ray crystal structure while the β-strand content is about 22% less estimated than the crystal structure. The refolded protein exhibited contents of α-helices and β-strands of 29.6% and 24.7% on average, respectively, very similar to those of the native protein. This suggests that the overall secondary structures were almost completely recovered after refolding. The slight differences in the fluorescence and CD spectra between the native and the refolded proteins might be due either to the existence of urea at a low concentration in the refolding solution or to slight imperfection of refolding. Reversibility of KSI folding was also assessed by a 100-fold dilution of the denatured protein and subsequent determination of enzyme activity. More than 95% of the activity was recovered after the refolding, indicating that the

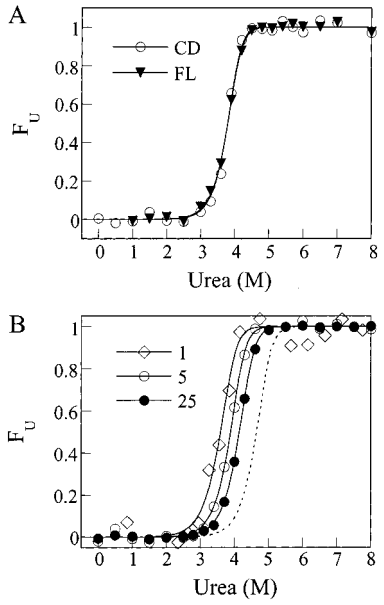

FIGURE 4: Unfolding equilibrium transition of KSI induced by urea. (A) Coincidence of the transition curves obtained from both fluorescence and CD measurements. The fluorescence intensity at 304 nm obtained after excitation at 275 nm and the molecular ellipticity at 222 nm were measured, respectively, for the protein at 15 μM in phosphate buffer containing urea at different concentrations. (B) Dependence of the equilibrium unfolding transition on the protein concentration. The unfolding transition was analyzed by fluorescence measurement at three different protein concentrations of 1, 5, and 25 μM. The dotted curve represents the predicted transition curve obtained for 1 mM KSI at which the NMR experiments were carried out. The *y*-axis represents the fraction of unfolded protein. The data points were fitted to eq 4 to obtain the transition curve, from which $\Delta G_U^{H_2O}$ and *m* were calculated to be ca. 22.0 and 4.0 kcal mol^{-1} M^{-1}, respectively.

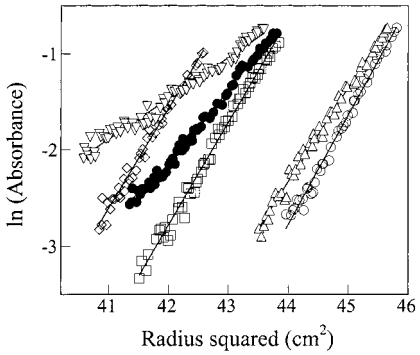

FIGURE 5: Sedimentation equilibrium analysis of KSI dissociation. Analytical ultracentrifugation data were displayed for the protein at 15 μM in phosphate buffer containing 0 (○), 1 (□), 2 (◇), 3 (△), 3.8 (●), and 5 M urea (▽), respectively. Data were collected at a rotor speed of 27 000 rpm and at 25 °C by measuring the absorbance at two different wavelengths, 230 and 280 nm. Data were shown in the format with the absorbance at 230 nm in the logarithmic scale versus the radius squared. The slopes for 0, 1, 2, 3, and 5 M urea were 1.14, 1.07, 1.04, 0.98, and 0.43, respectively. The slope for 3.8 M urea was between those obtained for the lower and higher urea concentrations.

refolded KSI retains almost the full catalytic function of the native enzyme (data not shown). The recovery of the activity by refolding was not diminished even after a prolonged time (24 h) of exposure to 7 M urea.

Equilibrium Unfolding. The equilibrium unfolding transition curve of KSI was obtained by measuring the fluorescence intensity at 304 nm and the CD ellipticity at 222 nm at different urea concentrations. Any significant changes in the intensities of fluorescence and ellipticity were not observed until the urea concentration reached 3 M (Figure 4A). In the range between 3 and 4.5 M urea, a drastic transition in the ellipticity and fluorescence intensities was observed. The transition curve was normalized by assuming that the fluorescence at 304 nm or the ellipticity at 222 nm for the native and unfolded states can be extrapolated linearly into the transition zone. There was no indication of any folding intermediates in the unfolding transition curve. The transition curves were almost coincident within experimental error for both fluorescence and CD measurements. These results strongly suggest that KSI folding can be described as a two-state model without any folded intermediate at equilibrium. When the spectroscopic data were fitted to the two-state model, the free energy difference, $\Delta G_U^{H_2O}$, and the *m* value were determined to be ca. 22.0 kcal·mol^{-1} and ca. 4.0 kcal·mol^{-1}·M^{-1}, respectively. The unfolding transition occurred at higher urea concentrations when the protein concentration was increased (Figure 4B). The transition midpoints were 3.60, 3.89, and 4.15 M for protein concentrations of 1, 5, and 25 μM, respectively. This observation is consistent with the two-state model describing the protein concentration dependence of the bimolecular reactions. The transition curve for 1 mM protein could be predicted to give the midpoint of 4.6 M urea by assuming that $\Delta G_U^{H_2O}$ and *m* values are 22.0 kcal·mol^{-1} and 4.0 kcal·mol^{-1}·M^{-1}, respectively. This prediction is based on the two-state model, in which $\Delta G_U^{H_2O}$ and *m* values should not be dependent upon the protein concentration (*35*).

Sedimentation Equilibrium Analysis of the Oligomeric State of KSI. The oligomeric state of KSI was analyzed by sedimentation equilibrium experiments performed at different urea concentrations. The absorbance in logarithmic scale was plotted against the radius squared in order to judge the linearities and relative slopes of the plots (Figure 5). The slopes for 0, 1, 2, and 3 M urea were 0.98−1.14, and the molecular weights were calculated utilizing the partial molar volume and solvent densities to give ca. 26 972 on average. This value agreed well with the calculated molecular weight, 26 788, for the dimer (*36*). The slope for 5 M urea was 0.42 and gave a molecular weight of ca. 13 000. This result suggests that KSI is dimeric at urea concentrations in the 0−3 M range with little evidence of dissociation while it was almost exclusively monomeric at urea concentrations higher than 5 M. However, at intermediate urea concentrations, 3.5−4.5 M, the molecular weight corresponded to the size between dimer and monomer. The data obtained at 3.8 M urea could be fitted to a mixture of dimers and monomers with the slope between those obtained for the lower and higher concentrations of urea.

Size-Exclusion Chromatography of KSI at Different Urea Concentrations. Size-exclusion chromatography was carried out to analyze the hydrodynamic properties of KSI at different urea conditions. Figure 6 shows the elution profiles of KSI after size-exclusion chromatography in various urea concentrations at 0, 4, and 6 M, respectively. At 0 and 6 M urea, only one species corresponding to the native dimer or the unfolded monomer could be observed. The unfolded monomer was eluted at earlier retention time than the native dimer probably due to its extended conformation. Meanwhile,

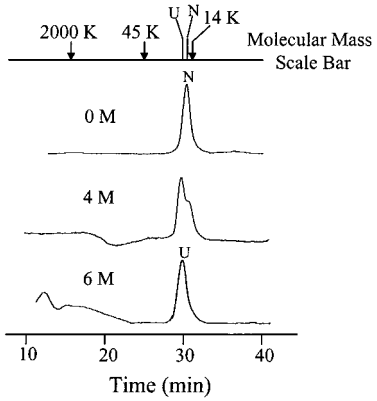

FIGURE 6: Gel-filtration chromatography of KSI at different urea concentrations. The protein was incubated in the presence of urea at 0, 4, and 6 M, respectively, for times longer than 48 h. The incubated protein was then loaded onto the column equilibrated with buffer containing 40 mM potassium phosphate, 1 mM EDTA, pH 7, and urea at the respective concentration. The flow rate was 0.4 mL/min, and the protein peak was monitored by the absorbance at 280 nm. N and U represent the peaks corresponding to the native and unfolded proteins, respectively. The molecular mass scale bar with blue-dextran, ovalbumin, and RNase A, whose masses are 2000, 45, and 14 kDa, respectively, was included. The positions of the N and U peaks are indicated to help the resolution of the peaks.

at 4 M urea, both peaks corresponding to the native dimer and the unfolded monomer were observed together, suggesting that two states coexist at this urea concentration. There was no peak for the folded monomer that would be eluted after the native dimer. This observation is also consistent with the two-state model supporting that there is no monomeric folded intermediate at equilibrium.

NMR Spectral Analysis. Two-dimensional ^{1}H-^{15}N HSQC spectra of KSI were obtained at different urea concentrations. In the absence of urea, the NMR peak positions were almost identical to those reported previously by Mildvan and coworkers (*37*) (Figure 7). Between 1 and 3 M urea, the resonance peaks were slightly shifted in positions probably due to the change of solvent conditions while significant positional shifts were observed between 3 and 6 M urea. At 6 M urea, the NMR spectrum exhibited a pattern of random coils with dense clustering of the resonance peaks. The spectrum obtained at 4.4 M urea exhibited a mixture of the resonance peaks observed in two respective spectra at 3 and 6 M urea. The 4.4 M urea concentration was tried since the unfolding transition midpioint was expected to occur near this concentration when the protein concentration was 1 mM (Figure 4B). The spectrum at 4.4 M urea could be reproduced by a simple addition of the spectra of the native and the unfolded proteins, supporting strongly that there is no folded intermediate at equilibrium.

Folding Kinetics. The time dependence of the fluorescence change of KSI was analyzed during the refolding process. The fluorescence intensity passed through a 295 nm cutoff filter after excitation at 275 nm increased during the period of the refolding process (Figure 8A). The refolding trace could be fitted by three exponential functions, suggesting that the KSI refolding consists of three kinetic phases. The trace exhibited a fast phase in the very early stage that was independent of the protein concentration with a rate constant of about 60 s^{-1} (Figure 8B). The fast phase was followed

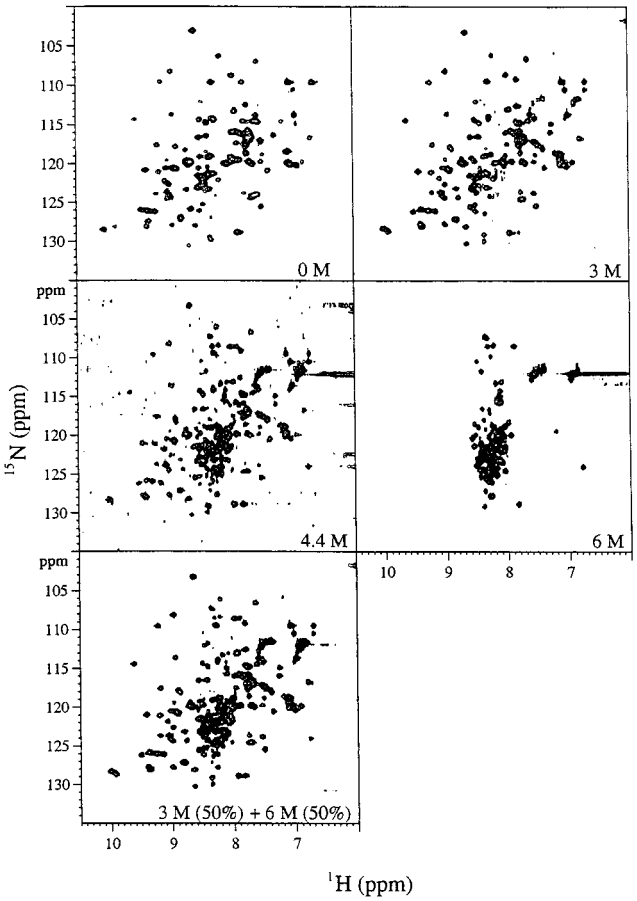

FIGURE 7: Two-dimensional ^{1}H-^{15}N HSQC spectra of KSI at different urea concentrations. The protein was incubated in the presence of urea at 0, 3, 4.4, and 6 M, respectively, longer than 48 h for equilibration. The HSQC spectra were obtained according to the protocol described under Experimental Procedures. The spectrum at the bottom was produced by the simple addition of the spectra obtained at 3 and 6 M urea using the equation: 0.5 × (spectrum at 3 M urea) + 0.5 × (spectrum at 6 M urea). The combined spectrum was almost identical to the observed one at 4.4 M urea, which would indicate no folded intermediate at equilibrium.

by an intermediate phase whose kinetic rate constant was dependent upon the protein concentration with a second-order rate constant of 5.4×10^{4} M^{-1}·s^{-1} (Figure 9A,B). This implies that the intermediate phase may represent the association step of the partially folded monomers. The first and second kinetic phases accounted for about 35% and 30% of the total fluorescence change, respectively (Figure 9C). The slow third kinetic phase was just marginally dependent upon the protein concentration and most likely was a unimolecular step with a rate constant of about 0.017 s^{-1}. This slow phase accounted for about 35% of the total fluorescence change.

The kinetics of KSI refolding were also analyzed by monitoring the ellipticity at 225 nm. During the dead time, the ellipticity change accounted for more than 83%, suggesting that the secondary structures form at a very early stage (Figure 10). The observed trace could be fitted by just one exponential function. The rate constant was 0.024 s^{-1}, which was comparable to that of the bimolecular step obtained from the fluorescence measurement. Thus, the dimerization step may contribute marginally to the formation of secondary structures. This implies that the monomeric

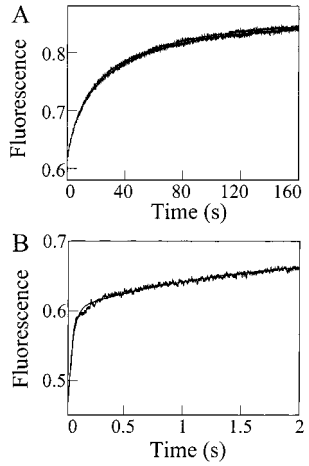

FIGURE 8: Refolding kinetics of KSI monitored by the fluorescence intensity. The denatured protein was induced for refolding by diluting the urea concentration from 8 to 0.62 M by use of a stopped-flow mixing apparatus. The fluorescence intensity passed through the 295 nm cutoff filter was monitored after excitation at 275 nm. The overall refolding trace (A) and the early phase of the refolding (B) are representatively shown for the concentration of protein at 4 μM. The solid line is the best fit for the refolding trace. The kinetic trace could be fitted nicely by three exponential functions.

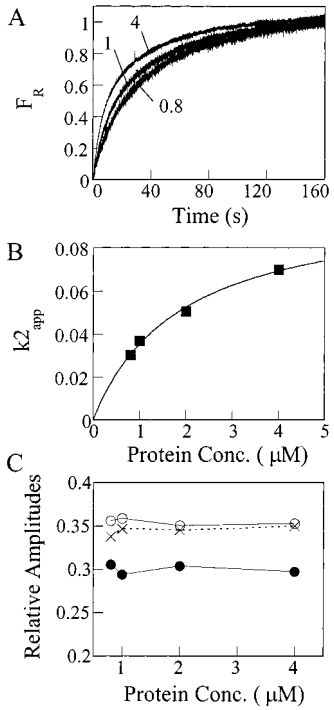

FIGURE 9: Dependence of the rate constants and the amplitudes of the three kinetic phases of KSI refolding on the protein concentration. (A) Kinetic traces of the refolding of KSI at 0.8, 1, and 4 μM, respectively. The *y*-axis represents the relative fluorescence change obtained by taking the fluorescences at 0 and ∞ s as 0 and 1, respectively. (B) Dependence of the apparent rate constant of the second kinetic phase ($k2_{app}$) on the protein concentration. The second-order rate constant was determined to be ca. 5.4×10^4 $M^{-1}\cdot s^{-1}$ in the low protein concentrations. (C) Dependence of the relative amplitudes of the three kinetic phases upon the protein concentration. The relative portions of the fast phase (○), the intermediate phase (●), and the slow phase (×) in the total amplitude are plotted against the protein concentration.

folding intermediate might form most of the secondary structures of the native state.

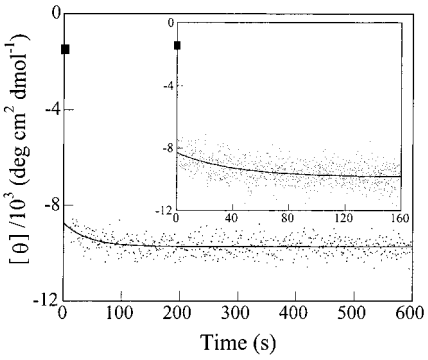

FIGURE 10: Kinetic trace of KSI monitored by the ellipticity change at 225 nm following a jump of urea concentration from 7 to 0.62 M. The protein concentration was 5 μM. Twelve traces were accumulated. The solid line is the best fit for the kinetic trace giving a rate constant of 0.024 s^{-1}. The *y*-axis represents the mean residue molar ellipticity. The inset represents the kinetic trace in the range 0−160 s. The initial ellipticity value (■) for denatured protein is indicated.

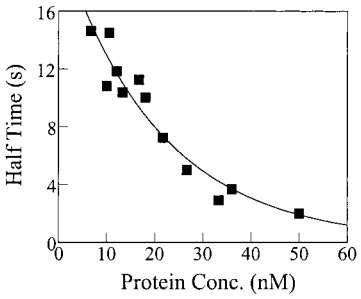

FIGURE 11: Dependence of half-life for recovery of the activity from the denatured state on the protein concentration. The denatured protein in 7 M urea was diluted into the assay buffer containing 5-AND to induce the refolding at various protein concentrations. The activity was measured during the refolding process by monitoring the absorbance at 248 nm. The time required to reach half of the final slope of the reactivation rate was taken as the half-life. The assay buffer used for refolding contains 34 mM potassium phosphate and 2.5 mM EDTA, pH 7.0. The final urea concentration was 0.023 M.

Activity of the KSI Monomer. The existence of the monomeric folding intermediate during the refolding process suggests a possibility of the active monomer. The catalytic activity of the KSI monomer was indirectly estimated from the analysis of the reactivation rate of the unfolded enzyme followed by refolding in a low urea concentration. Measurements of activity were followed 2 s after diluting the unfolded enzyme into the assay buffer without urea. The time required to reach half of the final slope of activity was analyzed against the protein concentration in the refolding buffer. The half-time was marginally dependent upon the protein concentration at concentrations above 30 nM but strongly dependent at lower protein concentrations (Figure 11). This result suggests that the KSI monomeric folding intermediate is not fully active. The monomeric intermediate, even if it contains mostly tertiary interactions, may lack the interactions stabilizing the structural integrity that would contribute to the efficient catalysis. The apparent rate constant for full activity recovery can be estimated from the half-times, which gave values of 0.03−0.25 s^{-1} in the 10−50 nM range of protein concentration. These values are considerably higher than the apparent rate constants of the bimolecular step, 0.03−0.07 s^{-1}, obtained from the refolding kinetic experiments at the higher protein concentrations. This implies that

KSI might have full activity at early stages of dimerization or partly folded monomers might have significant catalytic activity. The possibility for the occurrence of aggregated forms is not likely to be significant since activity was almost completely recovered after refolding at the micromolar protein concentrations (data not shown).

DISCUSSION

The equilibrium unfolding analysis suggests a highly cooperative two-state mechanism in which a folded dimer and an unfolded monomer are significantly populated at equilibrium. The structure of the KSI dimer (*9*, *10*) exhibits extensive interactions through hydrophobic contact among side chains in a region of antiparallel β-sheet from each monomer. Thus, the dissociation of monomers would be expected to result in the loss of the structural integrity of each monomer lacking the hydrophobic interactions that appear to stabilize the structure. The high value of $\Delta G_U^{H_2O}$ indicates that the dissociation of the KSI dimer is very difficult to occur. This is consistent with the previous observation that the KSI dimer was unusually stable to dissociation upon dilution (*22*−*24*). This high resistance to dissociation can reflect kinetic barriers to dissociation as well as thermodynamic stability. From these results, we can conclude that the KSI unfolding takes place by a mechanism in which the dimer is dissociated and unfolded simultaneously without any significant amount of a folded monomeric intermediate being populated.

On the basis of structural considerations, however, it seems unlikely that KSI undergoes the refolding process from unfolded monomers to a folded dimer in a single kinetic step. The kinetic analysis revealed that the KSI refolding process seems to consist of a fast first-order process followed by a second-order process and a slow first-order process. This implies that there is a monomeric folding intermediate before the association step. The KSI folding is thus likely to be a process in which the monomer folds to its proper conformation to form a monomeric folding intermediate retaining partially native interactions prior to the dimeric interaction. The monomers may collide with each other in a partially folded state to form a dimeric intermediate, which then proceeds to form the native dimer via one or more unimolecular folding steps. Thus, a simple model for the KSI folding can be proposed as follows:

$$2U \xrightarrow[(60\ s^{-1})]{\text{fast}} 2I \xrightarrow[(5.4 \times 10^4\ M^{-1}\cdot s^{-1})]{\text{dimerization}} I'_2 \xrightarrow[(0.017\ s^{-1})]{\text{slow}} N_2$$

where U, I, I'_2, and N_2 represent the unfolded monomer, the partially folded monomeric intermediate, the dimeric intermediate, and the folded dimer, respectively, and the rate constants represent the values obtained at 0.62 M urea. The above scheme suggests two folding intermediates, I and I'_2, that were not detected in equilibrium unfolding experiments. The last step from I'_2 to N_2 might represent unimolecular steps such as cis-trans isomerizations of prolines. The *C. testosteroni* KSI contains five proline residues per monomer. They form peptide bonds with trans configurations in the native state except one peptide bond of Asp38−Pro39. The proline isomerization might occur either in the unfolded monomer before association into the dimer or in the dimeric intermediate after association.

The structure of the monomeric folding intermediate is not clear. Since about 35% of the fluorescence change occurred in the fast phase (Figure 9C), the monomeric folding intermediate is expected to form much of the native tertiary interactions. The *C. testosteroni* KSI does not contain tryptophans, but instead it contains two tyrosine residues, Tyr14 and Tyr55, in the highly apolar active site that have strong fluorescence intensity (*38*). The increase of fluorescence intensity during the refolding process might represent the internalization of the tyrosine residues into the hydrophobic active site. The monomeric folding intermediate should also have hydrophobic patches exposed to polar solvent in advance to make a contact with the partner molecule. This kind of conformation would be very unstable since most hydrophobic residues have a tendency to get into the interior of proteins. The three-dimensional structure of KSI is distinctive in that a number of hydrophobic residues are located in the active site, forming the hydrophobic active-site cavity to bind apolar steroid substrates. The active-site cavity allows a few ordered water molecules (*10*), and the calculation of the dielectric constant gave the value of 18 for the deep active-site area (*38*). Therefore, the internalization of the apolar active-site residues to form the active-site cavity would be likely to be a driving force for the folding of KSI to generate the monomeric intermediate, which would be accompanied by the exposure of some hydrophobic residues to the dimeric interface. This speculation is consistent with the abrupt fluorescence change observed in the fast phase that can originate only from the internalization of the active-site tyrosine residues into the hydrophobic environment.

The second-order rate constant for KSI dimerization turns out to be in the range of values for subunit association reported previously (*39*). The constant is comparable to or severalfold lower than those of other dimeric proteins. In rabbit triosephosphate isomerase, the rate constant was $3 \times 10^5\ M^{-1}\ s^{-1}$ at 0 °C (*40*). Human glutathione transferase A1-1 exhibited a dimerization rate of $4.8 \times 10^5\ M^{-1}\ s^{-1}$ at 1 M urea and 15 °C (*41*). The bimolecular rate constant for the Arc repressor was in the range from 5×10^6 to $2 \times 10^7\ M^{-1}\ s^{-1}$ (*42*). The ellipticity change at 225 nm during refolding reflects that more than 83% of the secondary structures may form in the burst phase during the dead time (Figure 10). This suggests that most native secondary structures might be generated prior to the internalization of the tyrosine residues. At a very early stage, KSI may form partly amphipathic α-helices, which may come together with the orientations of the hydrophobic side inward to surround the active site, resulting in the stable α-helices. Given that β-sheet formation is relatively a late event, the dimerization may lead to the complete formation of the interface β-sheets. It would be possible that the formation of the hydrophobic active site may draw the peptide strands together to form the β-sheet since the β-sheet is responsible for one side of the hydrophobic active site. Our mutagenesis studies also suggest that the interface hydrogen bonds are important for the dimerization (Nam and Choi, unpublished data).

The proposed folding mechanism for KSI is similar to that for *E. coli* Trp repressor, in which the monomers partially fold prior to association (*19*, *43*). Such partially folded monomers contain some weakly stable helices with open hydrophobic surfaces to facilitate the association of the monomers. Human glutathione transferase A1-1 (*41*) and

triosephosphate isomerase (*44*) also form a structured monomer prior to dimerization. In contrast, extensive studies on the folding mechanism of P22 Arc repressor revealed that the monomers do not have significant structure prior to their association (*45*, *46*). The folding mechanism of a small 30 amino acid domain near the C-terminus of p53, called p53tet (*47*), is also similar to that of P22 Arc repressor since the first folding stage is the dimerization occurring concurrently with association of unstructured monomers (*21*). Taking these examples into consideration, the relationship between dimerization and protein folding is hard to generalize (*17*). Nevertheless, these studies will provide valuable insights into the roles of dimerization in the folding of dimeric proteins.

In conclusion, the KSI folding is almost completely reversible. It could be described as a two-state mechanism of a folded dimer and an unfolded monomer without any equilibrium folding intermediate. The dimerization plays an essential role in maintaining the conformational stability of KSI and contributes to the full activity recovery. The kinetic analysis of refolding revealed that there might be a monomeric folding intermediate retaining partially native tertiary interactions and most of the native secondary structures. Much more work is required for understanding the KSI refolding mechanism with extensive studies on the kinetics of unfolding and refolding to clarify whether KSI follows the three consecutive refolding steps. Urea dependence analysis of the folding kinetics combined with mutational studies will be valuable in dissecting the folding mechanism and in identifying interactions that are important for stabilizing the initial monomeric or dimeric folding intermediate.

ACKNOWLEDGMENT

We are thankful to Dr. Hyun Mee Kim at the National Instrumentation Center for Environmental Management for help with the analytical ultracentrifugation experiments.

REFERENCES

1. Batzold, F. H., Benson, A. M., Covey, D. F., Robinson, C. H., and Talalay, P. (1976) *Adv. Enzyme Regul. 14*, 243−267.
2. Pollack, R. M., Zeng, B., Mack, J. P. G., and Eldin, S. (1989) *J. Am. Chem. Soc. 111*, 6419−6423.
3. Wang, S.-F., Kawahara, F. S., and Talalay, P. (1963) *J. Biol. Chem. 238*, 576−585.
4. Pollack, R. M., Mack, J. P. G., and Eldin, S. (1987) *J. Am. Chem. Soc. 109*, 5048−5050.
5. Xue, L., Kuliopulos, A., Mildvan, A. S., and Talalay, P. (1991) *Biochemistry 30*, 4991−4997.
6. Hawkinson, D. C., Eames, T. C., and Pollack, R. M. (1991) *Biochemistry 30*, 10849−10858.
7. Hawkinson, D. C., Pollack, R. M., and Ambulos, N. P., Jr. (1994) *Biochemistry 33*, 12172−12183.
8. Kim, S. W., Cha, S.-S., Cho, H.-S., Kim, J.-S., Ha, N.-C., Cho, M.-J., Joo, S., Kim, K.-K., Choi, K. Y., and Oh, B.-H. (1997) *Biochemistry 36*, 14030−14036.
9. Wu, Z. R., Ebrahimian, S., Zawrotny, M. E., Thornburg, L. D., Perez-Alvarado, G. C., Brothers, P., Pollack, R. M., and Summers, M. F. (1997) *Science 276*, 415−418.
10. Cho, H.-S., Choi, G., Choi, K. Y., and Oh, B.-H. (1998) *Biochemistry 37*, 8325−8330.
11. Massiah, M. A., Abeygunawardana, C., Gittis, A. G., and Mildvan, A. S. (1998) *Biochemistry 37*, 14701−14712.
12. Kraulis, P. J. (1991) *J. Appl. Crystallogr. 24*, 946−950.
13. Schliebs, W., Thanki, N., Jaenicke, R., and Wierenga, R. K. (1997) *Biochemistry 36*, 9655−9662.
14. Mainfroid, V., Mande, S. C., Hol, W. G. J., Martial, J. A., and Goraj, K. (1996) *Biochemistry 35*, 4110−4117.
15. Bertini, I., Piccoli, M., Viezzoli, M. S., Chiu, C. Y., and Mullenbach, G. T. (1994) *Eur. Biophys. J. 23*, 167−176.
16. Sauer, R. T., Milla, M. E., Waldburger, C. D., Brown, B. M., and Schildbach, J. F. (1996) *FASEB J. 10*, 42−48.
17. Shakhnovich, E. I. (1999) *Nat. Struct. Biol. 6*, 99−102.
18. Boldwin, R. L. (1996) *Proc. Natl. Acad. Sci. U.S.A. 93*, 2627−2628.
19. Gloss, L. M., and Matthews, C. R. (1998) *Biochemistry 45*, 16000−16010.
20. Milla, M. E., Brown, B. M., Waldburger, C. D., and Sauer, R. T. (1995) *Biochemistry 34*, 13914−13919.
21. Mateu, M., del Pino, M. S., and Fersht, A. (1999) *Nat. Struct. Biol. 6*, 190−198.
22. Tivol, W. F., Beckman, E. D., and Benisek, W. F. (1975) *J. Biol. Chem. 250*, 271−275.
23. Weintraub, H., Vincent, F., and Baulieu, E. E. (1973) *FEBS Lett. 37*, 82−88.
24. Benson, A. M., Suruda, A. J., and Talalay, P. (1975) *J. Biol. Chem. 250*, 276−280.
25. Copeland, R. A. (1993) in *Methods of protein analysis*: *a practical guide to laboratory protocols*, Chapman and Hall, New York.
26. Kim, S. W., Kim, C. Y., Benisek, W. F., and Choi, K. Y. (1994) *J. Bacteriol. 21*, 6672−6676.
27. Provencher, S. W., and Glockner, J. (1981) *Biochemistry 20*, 33−37.
28. Johnson, W. C. (1999) *Proteins*: *Struct., Funct., Genet. 35*, 307−312.
29. Mok, Y.-K., Gay, G. D. P., Butler, P. J., and Bycroft, M. (1996) *Protein Sci. 5*, 310−319.
30. Laue, T. M., Shah, B. D., Ridgeway, T. M., and Pelletier, S. L. (1992) in *Analytical Ultracentrifugation in Biochemistry and Polymer Science* (Harding, S. E., Rowe, A. J., and Horton, H. C., Eds.) p 90, The Royal Society of Chemistry, Cambridge, England.
31. Wishart, D. S., Bigam, C. G., Yao, J., Abilgaard, F., Dyson, H. J., Oldfield, E., Markley, J. L., and Sykes, B. D. (1995) *J. Biomol. NMR 6*, 135−140.
32. Kay, L. E., Keifer, P., and Saarinen, T. (1992) *J. Am. Chem. Soc. 114*, 10663−10665.
33. Shaka, A. J., Keeler, J., Frenkiel, T., and Freeman, R. (1983) *J. Magn. Reson. 52*, 335.
34. States, D. J., Haberkorn, R. A., and Ruben, D. J. (1982) *J. Magn. Reson. 48*, 286.
35. Bowie, J. U., and Sauer, R. T. (1989) *Biochemistry 28*, 7139−7143.
36. Benson, A. M., Jarabak, R., and Talalay, P. (1971) *J. Biol. Chem. 246*, 7514−7525.
37. Zhao, Q., Abeygunawardana, C., and Mildvan, A. S. (1997) *Biochemistry 36*, 3458−3472.
38. Li, Y.-K., Kuliopulos, A., Mildvan, A. S., and Talalay, P. (1993) *Biochemistry 32*, 1816−1824.
39. Jaenicke, R. (1987) *Prog. Biophys. Mol. Biol. 49*, 117−237.
40. Zabori, S., Rudolph, R., and Jaenicke, R. (1980) *Z. Naturforsch 35C*, 999−1004
41. Wallace, L. A., and Dirr, H. W. (1999) *Biochemistry 38*, 16686−16694.
42. Milla, M. E., and Sauer, R. T. (1994) *Biochemistry 33*, 1125−1133.
43. Gloss, L. M., and Matthews, C. R. (1998) *Biochemistry 45*, 15990−15999.
44. Rietveld, A. W. M., and Ferreira, S. T. (1998) *Biochemistry 37*, 933−937.
45. Walburger, C., Johnson, T., and Sauer, R. (1996) *Proc. Natl. Acad. Sci. U.S.A. 93*, 2629−2634.
46. Milla, M. E., Brown, B. M., Waldburger, C., and Sauer, R. T. (1995) *Biochemistry 34*, 13914−13919.
47. Jeffrey, P., Gorina, S., and Pavletich, N. (1995) *Science 267*, 1498−1502.

BI000872D